A Numerical Study on Surface-piercing Propellers using Sliding Mesh Method via Openfoam Software

A. Amini, N. M. Nouri*, S. Niazi, A. Abedi

School of Mechanical Engineering, Iran University of Science and Technology, Tehran, Iran

P A P E R   I N F O

A B S T R A C T

Surface-piercing propellers (SPP) are known as one of the most efficient propellers in marine sciences and maritime industries. In this study, different types of simulations were performed on an SPP in various rotational speeds in open water conditions, and a numerical study was also carried out on a particular type of such propellers. In fact the main purpose of this paper is comparing the simulation results with the experimental results from past in order to derive a trustable soultion for future works. For this purpose, the surface-piercing propeller was simulated by OpenFoam software (an open source software with high range of capabilities) in order to analyze the results. The performance curve was then plotted and compared with the ones from open water tests. In this case the turbulance model of K-Epsilon RNG was used which is capable of increasing Y+ to 300 which is monitored at the end of the simulation with the maximum amount of 315 and the average of 80. Results showed that the curves followed the same pattern and trends in the numerical study, and the report pointed to similar findings. In conclusion, it was proved that the sliding mesh method was a proper way for simulating propellers, particularly SPPs. The curves for thrust and torque coefficients of the SPP were also compared with the literature and the efficiency curve was plotted.

doi: *10.5829/ijee.2023.14.04.11*

INTRODUCTION

With the flourish of maritime transport in the past decades, the need to upgrade vessels has convinced researchers to seek methods to improve the efficiency of their propulsion systems. The most common propulsion system used in submarines are ordinary propellers, yet they suffer from the destructive phenomenon of cavitation at high speeds and lose their efficiency [1]. On the other hand, in super cavitation propellers, large cavity forms behind the propeller surface, and prevents its failure around the propeller and the destructive effects of cavitation. However, the biggest problem occurs during cavitation and before the formation of super cavitation [2]. Waterjets are also among the most widely used propulsion systems in high-speed systems, but a significant problem with these systems is ventilation when losing contact with the water surface, and they are

therefore suitable for speeds up to 70 knots and above. Below the speed of 70 knots, SPP propellers are suitable [3].

The parts in surface-piercing propellers have a sharp leading edge and a thick trailing edge, which helps break up the water surface, while contributing to its structural strength. Despite the numerous advantages of these propellers over other propulsion systems in high-speed conditions, they have the following disadvantages:
1. At low speeds, they have extremely low efficiency due to the high force resulting from drag force.
2. They are exposed to many transverse forces and momentums due to asymmetric loading.
3. High instantaneous stresses occur due to the impact of the sharp edge of the blades in contact with the water surface.
4. Finally, reliable tools are not available for their design and analysis [4].

*Corresponding Author Email: mnouri@iust.ac.ir (N. M. Nouri)

Olofsson [5] performed an experimental work on the B-841 propeller, providing them with the full performance of the propeller and the average and instantaneous results.

The first method of numerical analysis of propellers is considered to be Rankin momentum theory, which tries to model the fluid flow around the propeller by considering simplifying assumptions, such as assuming a fluid flow ideal and not considering friction drag. This method, nevertheless, was not suitable for designing propellers [6], and only expressed the functional characteristics of the propellers. Thus, the first and simplest method for designing propeller, namely the linear method, was developed under extensive research to design propellers using the Kota-Chukovsky relationship. However, this method only provided satisfactory results for propellers with high side ratios (aerial propellers), and often obtained incorrect results for marine propellers with low side ratios Furuya [7] also applied this method to surface-piercing propellers. The second method developed with the appearance of the line-up method was the surface-lift method, which replaced the propeller surface with a vortex plate and then calculated the lift from it. Yet this method was not able to provide relatively accurate results akin to the experimental results either. With its development and taking into account the blade thickness, Young and Kinnas [8] formed the boundary element method in 2004, in which the surface of the blade was covered with vortex networks, and by obtaining the function of the potential on the lattices and the application of Gauss-Green theory and weighted residual integrals, unknown factors such as pressure can be obtained. Nevertheless, this method also considers the turbulence created by the propeller to be non-viscous and non-rotational, and the use of empirical relationships was required.

It should be noted that all the mentioned relationships were first invented and used for surface-piercing propellers, and for their optimal use for SPP propellers, scientists such as Young and Kinnas [6], Furuya [7], and the like tried to enter the free surface effect and modeling. In such propellers, ventilation occurred on the propeller surface, the results of which were presented earlier, but as observed, none were able to fully model these effects and the complex fluid flow near the surface.

After these efforts and progress in computer science, researchers tried to solve the Navier-Stokes equations, one of the most complex equations in the world, and due to their complexity and nonlinearity, as well as the impossibility of analytical solution, they solved these equations through numerical approaches, and were able to analyze the viscose and cavitational behavior of fluid flows through the proposed methods. Moreover, Cavitation Analysis of Fluid Flow by Caponnetto [9] first used the RANS method in 2002 to numerically model these propellers, stating that due to the complex nature of the free surface (cavities and water spray) the accuracy of

the boundary element method was not acceptable. Caponnetto [9] represented the axis and checked his obtained results with the data by Olofsson [5] and Young's boundary element [8], which proved satisfactory, yet one of the problems with his work was the lack of sufficient details. After him, Himei [10] from Japan used this method to examine the semi-SPP propellers and the results obtained in this respect. He presented his study in more details, and compared his work with experimental data and vortex networking method, which of course was better suited to it, but the coefficient of torque and force in different directions at low advance coefficients did not match adequately, neither did his work consider the water level increase when the blades emerged the water. After all, Alimirzazadeh et al. [11] conducted a new and relatively complete work on these propellers, using innovations such as the use of a sliding mesh instead of a rotating reference. However, they did not study all flow patterns and the graphs of the force and torque coefficients in their results, neither did their work include part of the complete ventilation pattern. Yang et al. [8] analyzed the hydrodynamic performance of SPP via CFD (computational fluid dynamics) method. In his study, they concluded the decrease of effects of ventilation on pressure distribution along the radial direction. They also investigated the effect on artificial ventilation in performance improvement of surface piercing propeller. At the end Rad et al. [13] also studied the effect of immersion ratios of 33, 40,50 and 70% on ventilation of surface piercing propeller's performance via sliding mesh method. They also used VOF method for open water simulation. The propeller that he used was 841-B four blade propeller which the same as Olofsson's thesis [5].

In 2023, Jalili and Jalili [14] did some numerical analysis of airflow turbulence in two-phase cross flow. Jalili et al. [15] also did another study for helix angles and the pressure drop in non-cotinuous helical baffles in 2022. Main point of these studies which was used in this work were the amount of Y+ which was derived around 300 in two phase flow. Jalili et al. [16] also studied the usage of curved rectangular fin in 2022. They used several meshes in order to reach the optimum amount of grid independency. Also, Jalili et al. [17] also did another research on convective-conductive heat transfer in 2018 which the grid independency in their system.

Kamran et al. [19] used URANS method coupled with VOF and captured the interface of fluids. She reached a 40% change in thrust and torque coefficient via the changes in trailing edge shapes. She also did another research in 2022 [20] and used regression modeling and different geometrical parameteres reached 90% prediction adequacy based on different factors. Kamran et al. [21] compared all of her results based on the results derived from the test setup which she designed and built in 2022.

The present research conducted a numerical study in this respect, using the sliding mesh method and the OpenFoam software. Hence, not only were the results obtained under this approach offered in both experimental and non-experimental studies, but also certain simulation outcomes were presented using the mentioned software. Accordingly, in the first step, the sliding mesh method was used in order to obtain the functional coefficients of the propeller by defining a periodic area at the beginning. Then, a transient solver and periodic boundary conditions were set up. Finally, the time-dependent data samples were entered, and the mean values were then computed. Various values were considered for open water pressure based on an experimental approach. It must be emphasized that the flow in the present study was defined as incompressible and non-viscous. Furthermore, the results were compared with the experimental results, which showed an applicable agreement.

It is relevant to note that this study not only laid the groundwork for numerous further investigations in this field, and confirmed the application of the sliding mesh method for simulation of the surface-piercing propeller, but also offered different methods for the investigation of the SPP. In other words, the present study can serve as the basics of the production and experiment of various propellers.

HYDRODYNAMIC CHARACTERISTICS

Although the SPP has lower propulsion efficiency at speeds below 50 knots, there are several techniques to enhance this efficiency, and ventilation is considered as the most important one of such techniques. With regard to ventilation, dimensionless forms of the propeller characteristics, including thrust coefficient (K_T), torque coefficient (K_Q), advance coefficient J, and efficiency η, are considered as follows:

$$K_T = \frac{T}{\rho n^2 D^5} \qquad \text{Thrust Coefficient} \qquad (1)$$

$$K_Q = \frac{Q}{\rho n^2 D^5} \qquad \text{Torque Coefficient} \qquad (2)$$

$$J = \frac{V_a}{nD} \qquad \text{Advance Coefficient} \qquad (3)$$

$$\eta = \frac{K_T}{K_Q} . \frac{J}{2\pi} \qquad \text{Efficiency} \qquad (4)$$

where, D is the propeller diameter, n is the propeller rotational speed, V is the advance velocity, ρ is the fluid density.

DESCRIBING SIMULATION AND SLIDING MESH THEORY

There are different theories for the simulation of propellers. In momentum theory, a disk is used instead of

the propeller, and indeed, a part of the propeller is considered to be inspected. There are also some other methods, such as the lifting line method to be the simplest one for simulation. CFD techniques have been used more frequently in the past decade. There are different approaches, such as RANS, LED, DES, and DNS in CFD for the modeling and simulation. In simulations, there also exist several models, such as K-ε, K-ω, and RSM turbulence methods.

In the finite volume method, the evaluation part has two different place and time areas, so that both areas are expanded within their own special ways.

Data collection instruments
Figure 1 shows that node P is located in the middle of the cell, and the control volume is covered by some planes. The area vector S_f for each plane is normal to its plane.

The sliding mesh method which is used in this approach in used for computing unsteady flows in case of moving object based on the time-accurate solution. Sliding mesh method provides unsteady solution which is in a time-periodic manner and repeats periodically in a relation with the speed of the moving domain. The standard form of the transport equation for each scalar like φ is presented below:

$$\frac{\partial \rho\varphi}{\partial t} + \nabla.(\rho U \varphi) - \nabla.(\rho\Gamma_\varphi \nabla_\varphi) = S_\varphi(\varphi) \qquad (5)$$

This equation is a second-degree equation and in order to get some good results, it is necessary to extend the equation by integrating around node P:

$$\int_t^{t+\Delta t} [\frac{\partial}{\partial t} \int_{Vp} \rho\phi dV + \int_{Vp} \nabla.(\rho U \phi) dV - \int_{Vp} \nabla.(\rho\Gamma_\phi \varphi) dt = \int_t^{t+\Delta t} (\int_{Vp} S_\phi(\phi) dV) dt \qquad (6)$$

The SPP is a type of super cavitation propeller, which has better performance at high speeds compared to other propulsion systems. On the other hand, due to different forces and also vibrations, special conditions are needed for designing and manufacturing these certain propellers. The key factors effective in the flow around SPP propellers are entirely based on timing and also being multiphase.
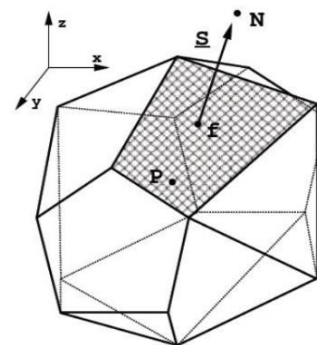

Figure 1. Finite volume element

The sliding mesh and multi-reference frame are two different techniques to simulate the propeller movement. The sliding mesh method is typically used due to its time dependency. Furthermore, it is capable of measuring sudden forces on a blade. Unfortunately, simulation via this technique is costly, and thus for simple simulations, the multi-reference frame (MRF) method is used; it is the simplest approach for modeling movements around circulation areas.

Equations used in two phase flows
There are different equations for two-phase flows, which can be used for the simulation of SPP in Eulerian methods to recognize the interface in order to solve a transport equation.

$$\alpha_L(\vec{x}.t) = \frac{V_L}{V} = \begin{matrix} 1 & \vec{x} \in Liquid \\ 0 < \alpha_L < 1 & \vec{x} \in Interface \\ 0 & \vec{x} \in Gas \end{matrix} \qquad (7)$$

It is noteworthy that the physical parameters are linearly changed as follows:

$$y = \alpha_L y_L + (1 - \alpha_L)y_G. y \in [\mu.\rho] \qquad (8)$$

The interface is moved by the flow. To keep the interface together, it is necessary to solve the transport equation as below:

$$\frac{\partial \alpha_L}{\partial t} + \vec{U}.\nabla\alpha_L = 0 \qquad (9)$$

The fluid volume function α is an expanded function and hence accurate patterns are needed to transport that. Since the boundaries of the solution were maintained in this study, the transport function was modified as below:

$$\frac{\partial \alpha_L}{\partial t} + \vec{U}.\nabla\alpha_L + \nabla.[\vec{U}_r\alpha_L(1 - \alpha_L)] = 0 \qquad (10)$$

Transpose term causes compression and higher resolution of the interface; unlike methods such as CICSAM and HRIC, adding this term terminates the need for a particular technique for that. Hence, the high compression speed is evaluated as follows:

$$\vec{U}_r = min(C_a|\vec{U}|.max(|\vec{U}|))\frac{\nabla\alpha_L}{|\nabla\alpha_L|} \qquad (11)$$

where $C_a = 0$ is the compression coefficient. It must be noted that this coefficient is added to cause more compression for the surface.
The Navier-Stokes equation for two-phase flows is presented as:

$$\frac{\partial(\rho\vec{U})}{\partial t} + \nabla.(\rho\vec{U}\vec{U}) = -\nabla P_{rgh} + \rho\vec{g} + \nabla.T + F_\sigma \qquad (12)$$

Both Newtonian and incompressible fluids are assumed. Therefore, the rate of the strain tensor is linearly related to the stress tensor, so the stress tensor is simplified as follows:

$$\nabla.T = \nabla.(\mu(\nabla\vec{U}^T + \nabla\vec{U})) = \nabla.(\mu\nabla\vec{U}) + (\nabla\vec{U}).\nabla\mu \qquad (13)$$

PROPELLER GEOMETRY

For the purposes of this study, a propeller with a diameter of 250mm and 4 blades was used. As shown in Table 1, the hub diameter is 85 millimeters, and the pitch is at a radius of 0.7, which equals 310 millimeters.
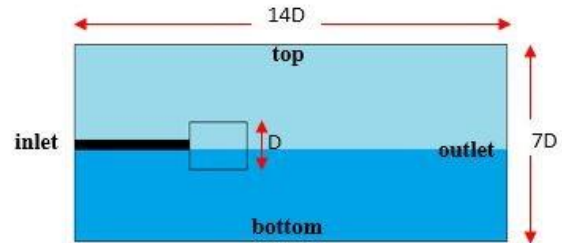
BOUNDARY CONDITIONS AND MESH

The software used in this paper is known as OpenFoam, capable of managing to solve different areas of a physical and chemical phenomenon. The main property of the software is the use of programming skills. The simulation area includes different sections, as displayed in Figure 2, such as wall boundaries (bottom), inlet, and outlet. As shown, the diameter of the propeller is indicated by D, the length of the tunnel is given by 14D, and the depth of water is shown by 3.5D. The boundary conditions of simulation in OpenFoam is stated in Table 2.

Regarding the inlet boundary conditions, it is worth noting that this problem was first considered as a water channel without a propeller, in the inlet boundary of half

Table 1. Model propeller specifications

Propeller Diameter	Hub Diameter	Pitch at Radius of 0.7	Number of Blades
250	85	310	4

Figure 2. Physics of simulation

Table 2. Boundary conditions of simulation in OpenFoam

	P	U
Inlet	Zero Gradient	Constant
Outlet	Constant	Open Boundary
Top	Constant	Open Boundary
Bottom	Zero Gradient	Slip
Front	Zero Gradient	Zero Gradient
Back	Zero Gradient	Zero Gradient
Propellet	Zero Gradient	No Slip

of the channel with water with a constant velocity and constant pressure gradient, and for the upper half, which is usually air, in the form of a pressure gradient It was assumed constant that we reach a water channel after convergence and then these conditions are considered as initial conditions when the propeller and rotating region are added. The propeller shaft was also simulated in such a way that its surface was simulated as zero gradient and its drag effect was added in the calculation, but the rotating property of the shaft was not considered in this problem.

In general, the geometry is divided into two rotating areas (the cylinder around the propeller) and non-rotating outside the cylinder. Except for the cylindrical area around the propeller, the rest of the areas are meshed in an organized manner, which causes high quality meshing, but the cylindrical area around the propeller is meshed in an unorganized manner by ICEM software and in the interface areas. Overall mesh size of the cube is 40×20×20, which is reduced to 10 times the mesh in the areas of the interface at the height of D.

Meshing depends on the areas of simulation. In this paper, the sliding mesh method was used for the simulation. When a time-accurate solution for rotor-stator interaction (rather than a time-averaged solution) is desired, the sliding mesh model was used to compute the unsteady flow field. The sliding mesh model is the most accurate method for simulating flows in multiple moving reference frames and the most computationally demanding, as well. In this method, two or more cell zones are used (if the mesh is generated in each zone independently, mesh files need to be merged prior to the calculation). Each cell zone is bounded by at least one "interface zone", where it meets the opposing cell zone. The interface zones of adjacent cell zones are associated with one another to form a "mesh interface." The two cell zones will move relative to each other along the mesh interface.

Figure 3 shows the meshed propeller via sliding mesh method. The Meshed physics of simulation is illustrated in Figure 4. As shown in this figure, there were various regions in the present simulation with simple and complicated geometries, and therefore, a mixture of organized and non-organized meshing was considered. A propeller is a complicated zone, which has a non-organized mesh. Nonetheless, the rest of the areas were meshed with an organized method.

The Moving part is meshed in an unorganized manner by ICEM software and because in the sliding mesh relations, all the properties are transferred by the transfer relations between the two fixed and moving parts, so the cylindrical area is considered to be almost equal to the diameter of the propeller. Also, the distance of the first cell to the surface of the propeller is considered to be 0.1 mm, and this distance is first calculated by the relation Y+ related to the flow on a smooth surface, and considering Y+ equal to 100 and obtaining the distance of the first cell
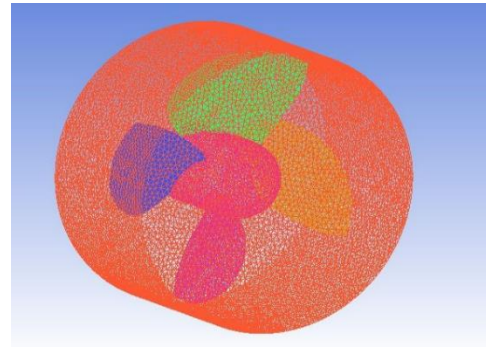

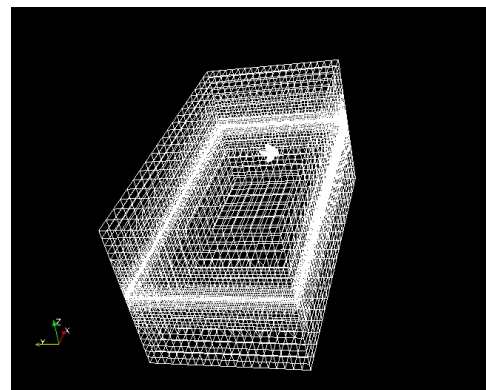**Figure 3.** Meshed propeller via sliding mesh method

Figure 4. Meshed physics of simulation

from this relation, first it has been estimated and then with an initial simulation we reached the desired number for the distance of the first cell. It should be noted that the entire boundary layer was not meshed and calculated because it required high computing power and was impossible in practice, so the boundary layer was calculated using the wall function and one of the reasons for using the K-epsilon RNG turbulence model. It was because of the ability to increase y plus up to 300.

TURBULENCE MODEL

K-epsilon is the best method for problems not influenced by boundary layer and separation effects. In this study, hence, K-epsilon RNG was employed in order to eliminate some issues near the wall. This model was developed by Yakut et al. [18]. To calculate the effects of small flow scales:

$$\frac{\partial}{\partial t}(\rho k) + \frac{\partial}{\partial x_i}(\rho k u_i) = \frac{\partial}{\partial x_j}\left[\left(\mu + \frac{\mu_t}{\sigma_k}\right)\frac{\partial k}{\partial x_j}\right] + P_k - \rho\varepsilon \tag{14}$$

$$\frac{\partial}{\partial t}(\rho\varepsilon) + \frac{\partial}{\partial x_i}(\rho\varepsilon u_i) = \frac{\partial}{\partial x_j}\left[\left(\mu + \frac{\mu_t}{\sigma_\varepsilon}\right)\frac{\partial\varepsilon}{\partial x_j}\right] + C_{1\varepsilon}\frac{\varepsilon}{k}P_k - C_{2\varepsilon}^*\rho\frac{\varepsilon^2}{k} \tag{15}$$

$$C_{2\varepsilon}^* = C_{2\varepsilon} + \frac{C_\mu \eta^3 (1-\eta/\eta_0)}{1+\beta\eta^3} \qquad (16)$$

$$\eta = Sk/\varepsilon \text{ and } S = (2S_{ij}S_{ij})^{1/2} \qquad (17)$$

where:
$C_\mu = 0.0845$
$\sigma_k = 0.7194$
$\sigma_\varepsilon = 0.7194$
$C_{\varepsilon 1} = 1.42$
$C_{2\varepsilon} = 1.68$
$\eta_0 = 4.38$
$\beta = 0.012$

SIMULATION RESULTS
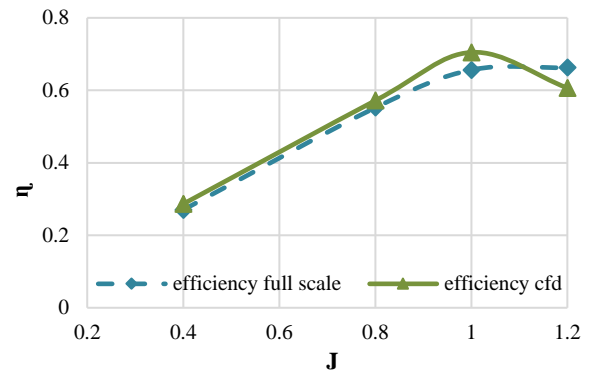
Simulation was performed in two different circulation speeds. For this purpose, the integral was used for instant data plus thrust and torque coefficient outcomes associated with the main model. Three different diagrams were reported from the OpenFoam software and compared with the full-scale results.

All of the results are plotted in Figures 5, 6, and 7. The results show that although there was an applicable agreement between the main model and the simulations, some discrepancies can be observed for low advance coefficients due to water spray and high vibration.
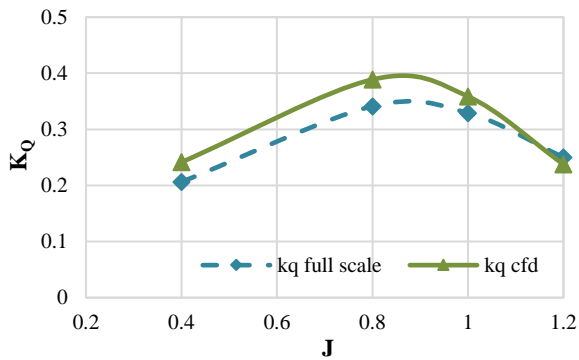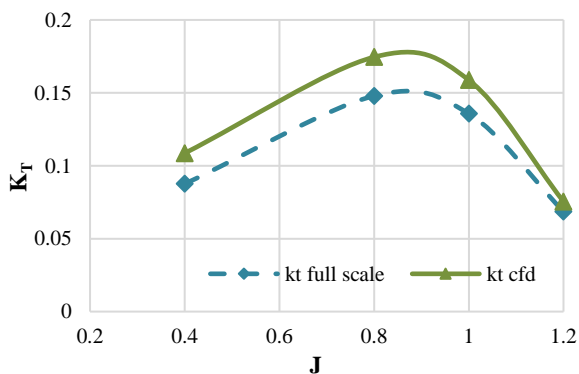

Figure 5. K_Q-J simulation diagram

Figure 6. K_T-J simulation diagram

Figure 7. η-J simulation diagram

As depicted in Figure 7, the efficiency of the propeller in both full scale and CFD design was similar to a large extent, which showed that the results of CFD simulation in OpenFoam will be reliable. There is a breaking point between two range of results near J=1.1, and water speed increases with the growth of J. At high speeds of water in a tunnel, errors increase, and the mentioned breaking point is the cause of these errors. Furthermore, the results show a perfect trend, which is akin to the full-scale results in the mentioned advance coefficients.

The main model of propellers tests were performed in a tunnel with a water speed of 6 (m/s). The tunnel dimensions were 16×7 (m) and 200 (m) length. A whole comparison between full-scale open water tests and CFD simulation is shown in Figures 5, 6, and 7. As for K_t, the results show that CFD simulation produced the highest values. The results are the same for K_Q; however, there was a different scenario for efficiency plotted in Figure 7. As can be observed, the efficiency of the CFD was higher than the main model at low speeds and J less than 1.

Not only did the thrust and torque coefficients have different amounts, but the current test model also presented a lower amount. Various scenarios can be claimed for this difference, such as a difference between the test model surface and the propeller main model, which would exert certain impacts on current results. Also, the effects of tunnel walls could cause vibration and produce some error. Full-scale propellers have no accurate data available for rates of angles in a shaft. In the present work, however, tests were performed by considering various angles, and some errors could be anticipated.

According to Table 3 and in order to optimize the results and the price of calculations, with an increase in mesh from 800,000 to 4.1 million, the maximum percentage of relative error decreased from 80% to 25%, which according to Figure 8, was attributed to hydrodynamic efficiency at advance coefficient of 0.4.
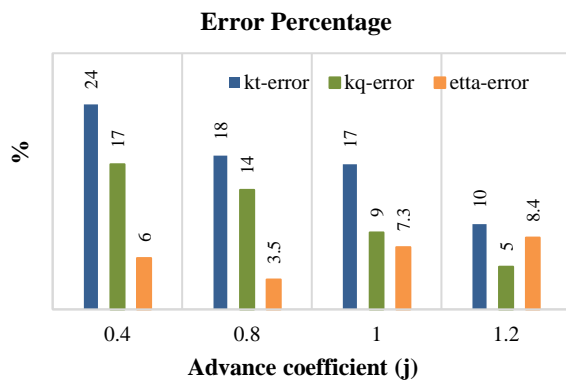
The contour of propeller at J=0.8 in one circulation is shown in Figure 9.

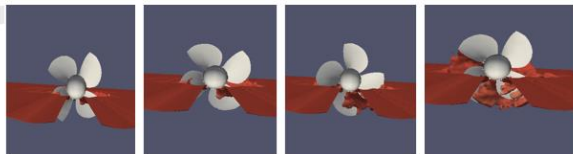The error rate is derived according to the following equation:

$$PercentageError = \left(\frac{CFDdata - FullScaleExperimentalData}{CFDdata}\right) \times 100 \tag{18}$$

Table 3. Mesh independency

Number of Meshes	Percentage of Error
800000	80%
2000000	57%
4100000	25%

Error Percentage

Figure 8. Error percentage between experimental and cfd analyses

Figure 9. Contour of propeller at J=0.8 in one circulation

CONCLUSION

Principally, there are two choices for propulsion systems on high-speed crafts: surface-piercing propellers and waterjets. Since for speeds above 70 knots, crafts tend to move out of water, waterjets cause numerous problems in the suction area, which is the main reason for the low efficiency in these types of propulsion systems.

Hence, in this research, the hydrodynamic performance of a particular SPP type was studied via OpenFoam software. The sliding mesh method was used for the simulation of the propeller movement, which was considered to be more accurate than MRF. The procedure followed the RANS method, along with the VOF model. In this work, the primary objective was to consider a new approach for the simulation of surface-piercing propellers, known as the sliding mesh. Since this method is used in many different studies, in order to have the inovation for this paper, Openfoam software (an open source software) was used for simulation, Consequently, the obtained results of K_Q, K_T and η were compared with those of experimental ones. The results indicated a maximum error of 7 % for efficiency, when approximately four million meshes were considered at an advance coefficient of 0.4. Furthermore, the results of the simulation via the sliding mesh method showed higher levels of the K_Q, K_T, and η than full-scale test ones.

These results show that this method of simulation is highly practical and can be used for different areas in marine studies, and surface-piercing propellers in particular. It also showed that Openfoam software is a highly efficient software for running simulation with cheaper hardware needs. Meanwhile, it is possible to reduce the error by increasing the advance coefficient. Moreover, different reasons have been identified for the increase of error at low advance coefficients, such as maladjustment of open water surface in low advance coefficients.

The following areas can be proposed for future work in this respect:

- Reviewing the propeller operation at off-design conditions as it is essential to note that different studies have been made over previous decades;
- Adding a cavitation model for low advance coefficients, which can be performed both as experimental and simulation. It is noteworthy that with the success of the sliding mesh method in this paper, it can be used in future works;
- Increasing the efficiency of SPP via different methods, such as ventilation, in which a setup can be made for experimental studies in this area;
- Reviewing the propeller performance in off-design points.

CONFLICT OF INTEREST

The authors declare that they have no conflict of interest.

REFERENCES

1   Faltinsen, O.M., 2005. Hydrodynamics of high-speed marine vehicles. Cambridge University Press. Doi: 10.1017/CBO9780511546068

2   Parker, J.R., 2017. Design and numerical analysis of an unconventional surface-piercing propeller for improved performance at low and high speeds (Doctoral Dissertation,

Massachusetts Institute of Technology). http://hdl.handle.net/1721.1/111891

3   Young, Y.L., Savander, B.R., 2011. Numerical analysis of large-scale surface-piercing propellers. *Ocean Engineering*, 38(13), pp. 1368-1381. Doi: 10.1016/j.oceaneng.2011.05.019

4   Peterson, D., 2005. Surface-piercing propeller performance. Naval Postgraduate School, Monterey, California. http://hdl.handle.net/10945/2046

5   Olofsson, N., 1996. Force and flow characteristics of a partially submerged propeller. Ph.D. Thesis, Chalmers University of Technology.

6   Young, Y.L., & Kinnas, S.A., 2001. A BEM for the prediction of unsteady midchord face and/or back propeller cavitation. *Journal of Fluids Engineering*, 123(2), pp. 311-319. Doi: 10.1115/1.1363611

7   Furuya, O., 1985. A performance-prediction theory for partially submerged ventilated propellers. *Journal of Fluid Mechanics*, 151, pp. 311-335. Doi: 10.1017/S0022112085000982

8   Young, Y.L. and Kinnas. S.A., 2004. Performance prediction of surface-piercing propellers. *Journal of Ship Research*, 48(4), pp. 288–304. Doi: 10.5957/jsr.2004.48.4.288

9   Caponnetto, M., 2003. RANSE simulations of surface piercing propellers. In Proceedings of the 6th Numerical Towing Tank Symposium.

10 Himei, K., 2013. Numerical analysis of unsteady open water characteristics of surface piercing propeller. In Third International Symposium on Marine Propulsors smp (Vol. 13, pp. 292-297). Doi: 10.3390/w11102015

11 Alimirzazadeh, S., Roshan, S.Z., Seif, M.S., 2016. Unsteady RANS simulation of a surface-piercing propeller in oblique flow. *Applied Ocean Research*, 56, pp. 79-91. Doi: 10.1017/CBO9780511546068

12 Yang, D., Ren, Z., Guo, Z. and Gao, Z., 2018. Numerical analysis on the hydrodynamic performance of an artificially ventilated surface-piercing propeller. *Water*, 10(11), p.1499. Doi: 10.3390/w10111499

13 Rad, R.G., Shafaghat, R. and Yousefi, R., 2019. Numerical investigation of the immersion ratio effects on ventilation phenomenon and also the performance of a surface piercing propeller. *Applied Ocean Research*, 89, pp. 251-260. Doi: 10.1016/j.apor.2019.05.024

14 Jalili, B. and Jalili, P., 2023. Numerical analysis of airflow turbulence intensity effect on liquid jet trajectory and breakup in two-phase cross flow. *Alexandria Engineering Journal*, 68, pp. 577-585. Doi: 10.1016/j.aej.2023.01.059

15 Jalili, P., Kazerani, K., Jalili, B. and Ganji, D.D., 2022. Investigation of thermal analysis and pressure drop in non-continuous helical baffle with different helix angles and hybrid nano-particles. *Case Studies in Thermal Engineering*, 36, p.102209. Doi: 10.1016/j.csite.2022.102209

16 Jalili, B., Aghaee, N., Jalili, P. and Ganji, D.D., 2022. Novel usage of the curved rectangular fin on the heat transfer of a double-pipe heat exchanger with a nanofluid. *Case Studies in Thermal Engineering*, 35, p.102086. Doi: 10.1016/j.csite.2022.102086

17 Jalili, P., Ganji, D.D. and Nourazar, S.S., 2018. Investigation of convective-conductive heat transfer in geothermal system. *Results in Physics*, 10, pp.568-587. Doi: 10.1016/j.rinp.2018.06.047

18 Yakut, R., Yakut, K., Yeşildal, F., Karabey, A., 2016. Experimental and numerical investigations of impingement air jet for a heat sink. *Procedia Engineering*, 157, pp. 3-12. Doi: 10.1016/j.proeng.2016.08.331

19 Kamran, M., Nouri, N.M. and Askarpour, H., 2022. Numerical Investigation of the Effect of Trailing Edge Shape on Surface-Piercing Propeller Performance. *Applied Ocean Research*, 125, p.103230. Doi: 10.1016/j.apor.2022.103230

20 Kamran, M. and Nouri, N.M., 2022. Regression Modeling of surface piercing propeller performance based on trailing edge geometrical parameters using CFD method. *Ocean Engineering*, 259, p.111752. Doi: 10.1016/j.oceaneng.2022.111752

21 Kamran, M. and Nouri, N.M., 2022. Model testing system for surface-piercing propellers in a water tunnel: Design and in situ calibration methodology. *Measurement*, 199, p.111200. Doi: 10.1016/j.measurement.2022.111200

Persian Abstract

چکیده

پروانه‌های نیمه مغروق (SPP) به عنوان یکی از کارآمدترین پروانه‌ها در علوم دریایی و صنایع دریایی شناخته می‌شوند. در این تحقیق انواع مختلفی از شبیه‌سازی‌ها بر روی یک SPP در سرعت‌های دورانی مختلف در شرایط آب آزاد انجام شد و یک مطالعه عددی نیز بر روی نوع خاصی از این پروانه‌ها انجام شد. در واقع هدف اصلی این مقاله مقایسه نتایج شبیه‌سازی با نتایج تجربی گذشته به منظور استخراج روش قابل اعتماد برای کارهای آینده است. برای این منظور، پروانه نیمه مغروق توسط نرم‌افزار OpenFoam (یک نرم‌افزار متن‌باز با قابلیت‌های فراوان) شبیه‌سازی شد و سپس منحنی عملکرد رسم شد و با نمونه‌های آزمایش‌های آب آزاد مقایسه شد. در این مورد از مدل توربولانس K-Epsilon RNG استفاده شد که قابلیت افزایش +Y را به ۳۰۰ دارد که در پایان شبیه‌سازی با حداکثر مقدار ۳۱۵ و میانگین ۸۰ پایش می‌شود. نتایج نشان داد که منحنی‌ها یکسان هستند، الگو و روند در مطالعه عددی و گزارش به یافته‌های مشابه اشاره کرد. در نتیجه، ثابت شد که روش Sliding Mesh روشی مناسب برای شبیه‌سازی پروانه‌ها، به ویژه SPP ها است. منحنی‌های ضرایب رانش و گشتاور SPP نیز با گزارش مقایسه شد و منحنی عملکرد رسم شد.